

## Article

# A Taste Bud Organoid-Based Microelectrode Array Biosensor for Taste Sensing

Shuge Liu <sup>1,2</sup> , Ping Zhu <sup>1,2</sup>, Yulan Tian <sup>1,2</sup>, Yating Chen <sup>1,2</sup>, Yage Liu <sup>1,2</sup>, Miaomiao Wang <sup>1,2</sup>, Wei Chen <sup>1,2</sup>, Liping Du <sup>1,2,\*</sup> and Chunsheng Wu <sup>1,2,\*</sup> 

- <sup>1</sup> Department of Biophysics, Institute of Medical Engineering, School of Basic Medical Sciences, Health Science Center, Xi'an Jiaotong University, Xi'an 710061, China; 4120115012@stu.xjtu.edu.cn (S.L.); jewel121@stu.xjtu.edu.cn (P.Z.); cnyulantian@stu.xjtu.edu.cn (Y.T.); ytc20201011@stu.xjtu.edu.cn (Y.C.); liuyage@stu.xjtu.edu.cn (Y.L.); wmm15029418463@stu.xjtu.edu.cn (M.W.); weiwchen@xjtu.edu.cn (W.C.)
- <sup>2</sup> Key Laboratory of Environment and Genes Related to Diseases, Xi'an Jiaotong University, Ministry of Education of China, Xi'an 710061, China
- \* Correspondence: duliping@xjtu.edu.cn (L.D.); wuchunsheng@xjtu.edu.cn (C.W.)

**Abstract:** The biological taste system has the unique ability to detect taste substances. Biomaterials originating from a biological taste system have been recognized as ideal candidates to serve as sensitive elements in the development of taste-based biosensors. In this study, we developed a taste bud organoid-based biosensor for the research of taste sensation. Taste bud organoids prepared from newborn mice were cultured and loaded onto the surface of a 64-channel microelectrode array (MEA) chip to explore the electrophysiological changes upon taste; an MEA chip was used to simultaneously record multiple-neuron firing activities from taste bud organoids under different taste stimuli, which helped to reveal the role of taste buds in taste sensing. The obtained results show that taste cells separated from the taste epithelium grew well into spherical structures under 3D culture conditions. These structures were composed of multiple cells with obvious budding structures. Moreover, the multicellular spheres were seeded on a 64-channel microelectrode array and processed with different taste stimuli. It was indicated that the MEA chip could efficiently monitor the electrophysiological signals from taste bud organoids in response to various taste stimuli. This biosensor provides a new method for the study of taste sensations and taste bud functions.

**Keywords:** taste bud; organoid; biosensor; taste sensing; MEA



**Citation:** Liu, S.; Zhu, P.; Tian, Y.; Chen, Y.; Liu, Y.; Wang, M.; Chen, W.; Du, L.; Wu, C. A Taste Bud Organoid-Based Microelectrode Array Biosensor for Taste Sensing. *Chemosensors* **2022**, *10*, 208. <https://doi.org/10.3390/chemosensors10060208>

Academic Editor: Danila Moscone

Received: 14 April 2022

Accepted: 27 May 2022

Published: 2 June 2022

**Publisher's Note:** MDPI stays neutral with regard to jurisdictional claims in published maps and institutional affiliations.



**Copyright:** © 2022 by the authors. Licensee MDPI, Basel, Switzerland. This article is an open access article distributed under the terms and conditions of the Creative Commons Attribution (CC BY) license (<https://creativecommons.org/licenses/by/4.0/>).

## 1. Introduction

Taste is one of the basic and most important senses; types of tastes include sweetness, bitterness, umami, sourness, and saltiness. The development of a biological taste system is strictly regulated and must generate unique structures and functions that allow for taste sensations with high performance [1]. The biological taste system must be able to monitor the quality of food and avoid the intake of potentially dangerous substances. Loss of taste has a serious impact on the quality of life of patients; it has garnered more attention [2]. However, the underlying mechanisms of taste sensations are still not completely understood. It is essential to explore novel approaches for the research of taste sensations. In recent years, taste bud organoids have been successfully developed and applied to many fields, especially those related to biomedicine [3]. Taste bud organoids have the characteristics of strong usability, maneuverability, and high similarity to in vivo taste buds, providing great convenience in the research on taste functions and mechanisms. One emerging field in biomedicine involves the combination of organoids and sensors in developing organoid chips, showing promising prospects and potential applications in many fields [4,5]. One current research hotspot concerning organ chips involves the use of in vitro 3D cultured organoids to replace the traditional 2D cultured cells on the chip, which could provide more reliable research results than 2D culture methods.

Taste buds are specialized organs for taste sensations; they are capable of detecting and reporting oral irritation caused by chemicals such as alcohol and capsaicin, thereby one may likely avoid the intake of toxic and harmful foods. With in-depth studies on the coronavirus disease 2019, in addition to common symptoms (such as fever, cough, dyspnea, fatigue, and myalgia), loss of smell and taste is gradually being considered. A recent report showed that up to 41% of people infected with severe acute respiratory syndrome coronavirus 2 experience a loss of taste [6]. Although tricyclic antidepressants [7], clonazepam, or diazepam [8] are proven to be useful in improving abnormal taste sensations, there is still a lack of effective treatment interventions. Most research on taste has focused on the cellular level, revealing the expression of receptors and the transmission of taste signals [5,9,10]. Meanwhile, since most of the mechanisms that cause dysgeusia are unclear, there is no clear treatment plan for dysgeusia. Fortunately, taste bud organoids have been successfully established, providing powerful models for the research on taste sensing mechanisms as well as for physiology and pathology [11]. Taste bud organoids derived from mice of the oral mucositis model have been applied to study the therapeutic effects of drugs on taste loss [12]. It is a model based on a 3D in vitro cell culture system that is highly similar to the source tissues or organs in the body, which have been widely used in cancer research [13]. There is no doubt that organoid technology has greatly advanced the taste sensation mechanisms as well as the treatment of taste disorders.

Ion channels form the bases for cellular electrical signaling. In nerve cells,  $K^+$  and  $Na^+$  channels are important pathways for the generation and propagation of action potentials. The resting membrane potential of living cells is usually dominated by different concentrations of  $K^+$  ions inside and outside the cell. When an external stimulus occurs,  $Na^+$  mainly flows into the cells, and the membrane potential in the surrounding area starts to change from a resting potential to an action potential determined by the ratio of  $Na^+$  ions. Transient membrane depolarization subsequently triggers the slower opening of voltage-activated  $K^+$  channels, which then repolarizes the membrane to the resting potential [14]. Earlier studies demonstrated that taste cells have electrical properties comparable to those of neurons. Patch clamp recordings showed that mammalian taste cells are electrically excited and can fire action potentials when stimulated by taste substances [15–18]. In rodents, voltage-gated  $Na^+$  and  $Ca^{2+}$  channels are involved in depolarization, whereas  $K^+$  and likely  $Cl^-$  channels participate in repolarization during an action potential. Taste buds contain three types of taste cells [19]. Two types of taste receptors—the T1Rs identified for sweet and umami (glutamate) stimulation and the T2Rs for bitter stimulation—are coupled to the same downstream signaling effectors, including  $G\beta\gamma$  activation of  $PLC\beta 2$ ,  $IP_3$ -mediated  $Ca^{2+}$  transfer from the internal storage release of the cells, and  $Ca^{2+}$ -dependent activation of the monovalent selective cation channel TrpM5. These events lead to membrane depolarization and action potentials that activate taste afferents [20–22]. For the detection of taste cell membrane potential, a variety of bioelectronic devices have been developed by using taste cells or tissues [23,24], taste receptors [25], and heterologous expressions of taste receptor proteins [26] as sensitive elements. The transducers include microelectrode arrays [24], field-effect transistors [27], light-addressable potential sensors [23], and quartz crystal microbalance devices [28].

A microelectrode array (MEA) records extracellular electrical activities of cultured excitable cells or tissues from multiple recording sites [24] and there are many different forms. For example, multi-transistor, microelectrode, multielectrode, micro-nail, capacitive-coupled, and 3D structures are used as transducers of MEA. According to the type of substrate, MEAs are mainly categorized into active arrays, passive arrays, silicon arrays, or complementary metal-oxide semiconductor arrays. In contrast, needle-type probes and polytrodes are divided according to the shape of the device or the implantable array. A 3D probe records nerve signals sharply. Studies based on multiple flow channels [29], flexible materials of parylene-C [30], and wireless light [31] have demonstrated the use of needle probes. Polytrodes are high-density electrode arrays designed to record from large numbers of neurons [32]. On the other hand, MEA mainly includes in vivo MEA,

and in vitro MEA, according to the applications [33]. For the signal recorded by MEAs, bandpass filtering is usually performed first [34]. Bandpass filters are further divided into narrowband filters (300–3000 Hz) and broadband filters (1–7000 Hz). It is a common practice to use a wideband filter to record the data, and then use a narrowband filter to extract the spike timing information, which considers exactly when spikes occur within the time window [33]. After the spike signals of the taste cells are detected, there are two commonly used analysis methods. One is based on creating spike templates and then performing template matching. Another one usually relies on feature extraction and clustering, using both the spike shape and the estimated location of the event [35]. The next step is to group according to the spike shape, which is called spike sorting. The main methods used are the principal component analysis [36] and wavelet transform [37]. The earliest use of MEAs involved recording electrical signal changes in chicken heart cells under pulsed amplitudes [38]. Since then, the application of MEAs has rapidly developed [39,40]. At present, bioelectronic devices for taste detection have been developed based on taste cells or tissues [23,24], taste receptors [25], and taste receptor proteins prepared from heterologous expression systems [26]. Among them, MEA was one of the most important transducers due to its decisive advantages, such as high-throughput recording, high time resolution, and high quality of signals [24]. Our literature review showed no reports on the combined taste bud organoids with MEA chips for the development of taste-based biosensors.

Therefore, in the present study, we aimed to develop a taste bud organoid-based biosensor for the research of taste sensation. Taste bud organoids prepared from newborn mice were cultured and loaded onto the surface of a 64-channel MEA chip to explore the electrophysiological changes upon taste. An MEA chip was used to simultaneously record multiple-neuron firing activities from taste bud organoids under different taste stimuli. We recorded and discriminated the extracellular potentials of the taste receptor cells in taste bud organoids in response to basic taste qualities with the MEA–organoid hybrid biosensor. The obtained results suggest that it would help to reveal the spatiotemporal information of early taste sensing for the taste sensation and, thus, could potentially contribute to demonstrating the role of taste buds in taste sensing. It is worth noting that the MEA chips and taste bud organoids used in this study only demonstrate the technical feasibility of this novel approach for taste sensation mechanisms.

## 2. Materials and Methods

### 2.1. Preparation of Taste Bud Organoids

The experimental animals were 7-day-old C57BL/6J neonatal mice (Laboratory Animal Center of Xi'an Jiaotong University, Xi'an, China). After being anesthetized with urethane (25%, 5 mL/kg), the tongue tissues of mice were excised and the lingual epitheliums were stripped. Next, the epitheliums were minced and digested with 0.25% Trypsin-EDTA at 37 °C for 20 min. Then, the single cells were dissociated after filtering with a 40 µm filter and seeded in a 24-well ultra-low attachment culture plate. The culture medium (DMEM/F12, Gibco, 10565018, Waltham, MA, USA) was supplemented once every 3–4 days, which was made of a modified Hans Clever intestinal organoid medium, including R-spondin-1, Noggin, Jagged-1, Y27632, epidermal growth factor (EGF), N-2 supplement (a chemically-defined serum-free additive), and a B-27 serum-free supplement. After 10–15 days of culture, taste cell spheres were obtained and used for further experiments. The use of animals was approved by the Medical Ethics Committee of Xi'an Jiaotong University.

### 2.2. Immunostaining of Taste Bud Organoids

The cultured taste organoids were fixed with 4% (*w/v*) paraformaldehyde at room temperature for 30 min, permeabilized with 0.1% (*v/v*) Triton X-100 for 20 min, and finally blocked with 5% (*w/v*) bovine serum albumin (BSA) solution for 1 h. Then, they were incubated at 37 °C for 2 h with a primary antibody (GNAT3 Rabbit pAb, ABclonal, A15982, Wuhan, China; TRPM5 rabbit polyclonal antibody, Proteintech, 18027-1-AP, Chicago, MA, USA) and then with secondary antibody (Goat Anti-Rabbit IgG labeled with Flour594,

Affinity, S0008, Jiangsu, China) for 1 h, and finally with 4',6-diamidino-2-phenylindole (DAPI) for 20 min. Stained taste bud organoids were applied on glass slides and observed by a fluorescence microscope using a CARL ZEISS, AXIO Scope. A1 microscope (Carl Zeiss, Axio Scope A1, Germany).

### 2.3. MEA Setup and Measurement

In our work, 64-channel MEA chips (Multichannel system, USA), including 54 recording electrodes divided into 6 holes, were seeded with prepared taste bud organoids for a 24 h culture, allowing for attachment onto the chip surface. First, about 50  $\mu$ L of organoid suspension was added dropwise and placed at 37 °C for 30 min. This ensured that the spheroid was completely attached to the electrode. When taste stimulation substances were added, taste cells were depolarized, generating an action potential, which was then measured at the electrodes. Then, 150  $\mu$ L of taste bud organoid mediums were supplemented and incubated for 24 h. Finally, the MEA chip was fixed and linked with an MEA detection system to record the membrane potential with or without taste stimuli. With an Intan stimulation/recording system (Intan RHS2000, Los Angeles, CA, USA), the amplifier sampling rate was set at 30.0 kS/s (thousand dots per second). The elimination offset filter cutoff frequency was set to 1.00 Hz. The lower limit bandwidth of the amplifier was 0.1 Hz, and the upper limit bandwidth of the amplifier was 1000 Hz. Initially, when the basal discharge of taste cells was detected in the absence of stimuli, 10 mM of citric acid (KeyGEN BioTECH, KGF024, Jiangsu, China) and 100 mM of NaCl (Guanghua Sci-Tech Co., Ltd., 20140222, Guangdong, China) stimuli were added into the chamber in turn; the recording time was 5 min for each stimulus. Then, the cutoff frequency was set to 250 Hz to extract the spike timing information and analyze the change of the waveform under a Butterworth low-cut filter.

## 3. Results and Discussion

### 3.1. Preparation of Functional Taste Bud Organoids

To develop biosensors with high performance, it is essential (and favorable) to achieve functional biomaterials suitable to serve as sensitive elements for the detection of target signals. Within this context, the preparation of functional taste bud organoids is of great significance in the development of biosensors for taste sensations. For this, we prepared the taste bud organoids from the taste stem/progenitor cells isolated from the lingual epitheliums of neonatal mice using a 3D cell culture system. This system provides a well-defined microenvironment for the culture and differentiation of taste stem/progenitor cells, allowing for the cells to grow into 3D cell spheres. This makes it possible to generate taste bud organoids with structures and functions more similar to *in vivo* taste buds [41]. Organoids were generated from the whole tongue epithelium. We sorted progenitor/stem cells from neonatal mice. After culturing for 7–14 days using a taste organoid medium, the light micrographs of 7-day and 14-day cultured taste cell spheres are depicted in Figure 1a,b, respectively. In addition, Figure 1c shows an enlarged image of 1b in which the taste cell sphere had bud-like structures. From these micrographs, their diameters were observed to increase from ~300  $\mu$ m (Figure 1a,b) to 500  $\mu$ m (Figure 1c) with 3D structures. These 3D cell spheres were distributed evenly at a low density of 30–50 organoids per well. As a result, the spheres were easily suspended for use in further experiments. This greatly facilitates the transfer of these 3D cell spheres from the cell culture plate to the MEA chip surface.

Given the expanding morphologies of organoids, we hypothesized that mature taste cell markers may be expressed in them. Therefore, we performed immunofluorescent staining experiments on TRPM5 and GNAT3, which exist on the taste cell membrane and were considered features of taste buds [42,43]. On day 15, individual organoids were examined for incorporation of TRPM5 and GNAT3 primary antibodies after fixing with paraformaldehyde, permeabilizing with Triton X-100, and finally blocking with a BSA solution. Then, a secondary antibody with a red fluorophore was conjugated with the primary antibody to visualize the protein. DAPI is a fluorescent dye that binds strongly

to DNA; it was used to visualize cell nuclei in blue. There are three panels in Figure 1d,e. Of the three panels, the first column shows the expressions of the key proteins TRPM5 and GNAT3 (red) distributed on the spherical surface of taste bud organoids. The second column shows nuclear staining (to locate the location of the nucleus). The third column shows the results of merging the nucleus of the same organoid with images of proteins on the membranes. The results demonstrate the apparent TRPM5 and GNAT3 proteins presented on the cell membrane surrounding the nuclei (blue) of the taste bud cells. The above results also suggested that the prepared taste bud organoids consisted of type II taste receptor cells.

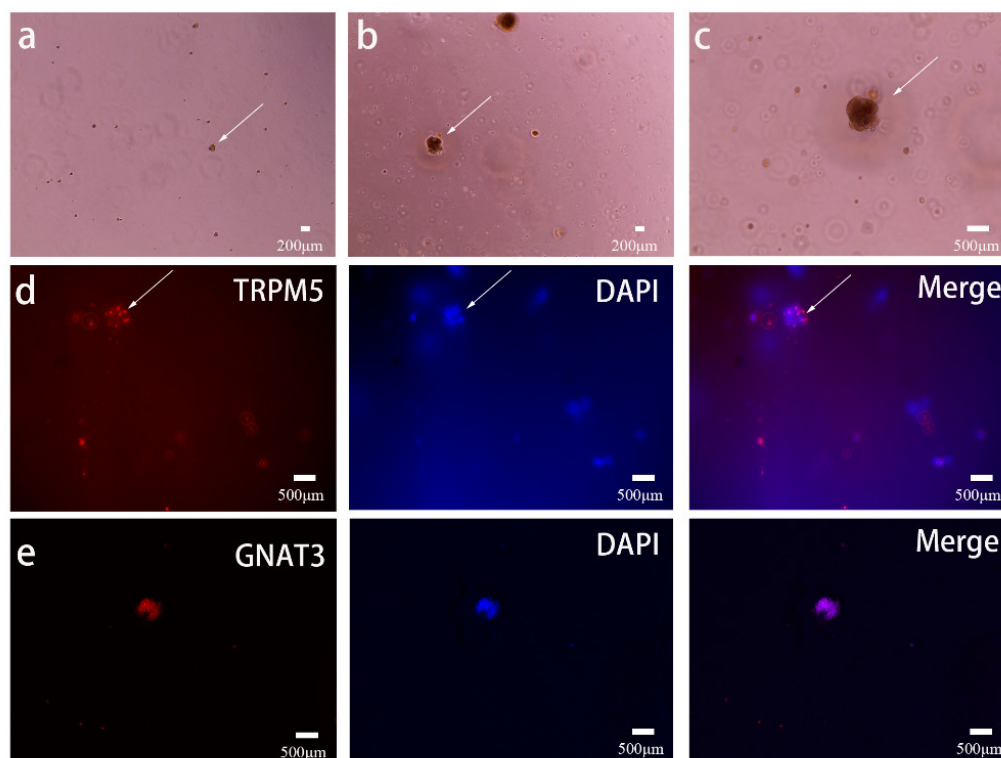


**Figure 1.** Light micrographs of (a) 7-day and (b) 14-day taste bud organoids prepared from neonatal mice. (c) A higher magnification image of (b). (d) Morphology and TRPM5 immunofluorescence staining of taste bud organoids cultured for 15 days using a TRPM5 rabbit polyclonal antibody (left) and DAPI fluorescent dye (middle). The right panel is a merged image of the left and middle. (e) GNAT3 immunofluorescence staining of taste bud organoids cultured for 15 days using GNAT3 Rabbit antibody (left) and DAPI fluorescent dye (middle). The right panel is a merged image of the left and middle.

To further investigate the growth of taste bud organoids, the sizes of 3D cell spheres at different growth days were recorded and compared. We first took pictures of the taste cell spheroids in each well, then used imageJ software to manually measure the diameters of the spheroids, and finally imported the data into GraphPad Prism 8.0 to obtain statistical results of different particle sizes at different culture days. The average diameter of 3D cell spheres increased rapidly with the growth time and reached a peak on the ninth day (Figure 2a). The average diameter of 3D cell spheres decreased slightly over time. This was probably due to inadequate nutrition supply to the center of the 3D cell spheres caused by the rapid volume increase of 3D cell spheres. As a result, the sizes of the prepared taste bud organoids were limited by the efficiency of the nutrition supply from the surface to the center of the 3D cell spheres. These results indicated that a 9-day growth was optimum for the preparation of taste bud organoids with optimal sizes. This hypothesis is proven by the results shown in Figure 2b, which shows the number distributions of different diameters of 3D cell spheres at different growth stages. The results revealed that the most suitable

growth time for cell spheroids was 9 days. During this period, the number of spheroids of all sizes was highest on day 9. It was suggested that the optimal sizes of taste bud organoids could be 300  $\mu\text{m}$ , which makes it possible to prepare taste bud organoids with identical sizes. It is important to develop biosensors with stable and identical performances. The obtained results lead us to conclude that the prepared taste bud organoids are suitable for further experiments—to develop taste bud organoid-based biosensors and investigate their responsive capabilities to various taste stimuli.

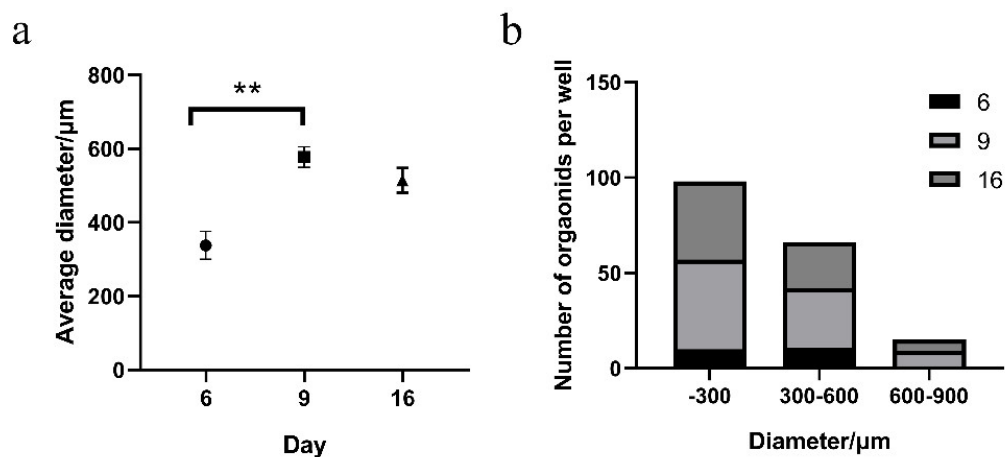


**Figure 2.** Particle size statistics of taste bud organoids at different growth days. (a) The average diameter of taste bud organoids on the 6th, 9th, and 16th day. All data represent the mean  $\pm$  standard error of the mean (S.E.M.) and are shown in a histogram. \*\*  $p < 0.01$  is considered as significant difference, Student's t-test. (b) Different particle size distributions of taste bud organoids at different growth days.

### 3.2. Coupling of Taste Bud Organoids with the MEA Chip

The coupling of sensitive elements with transducers is of great importance to the performance of biosensors. In this study, the prepared functional taste bud organoids were utilized as sensitive elements for the development of biosensors. We used 64-channel MEA chips as transducers for the membrane potential recordings from taste bud organoids under various taste stimuli. Thus, it is crucial to achieve high-efficient coupling between taste bud organoids and MEA chips. For this, the prepared taste bud organoids were transferred from the 3D cell culture system to the surface of an MEA chip that was sterilized before use. In addition, taste bud organoids were incubated on the surface of the MEA chip for 24 h, which allowed for good growth and good attachment of bud organoids onto the surface of the MEA chip. Moreover, taste bud spheroids were centrifuged before being transferred to the surface of the MEA chip, which increased the concentrations of taste bud organoids and, consequently, could increase the probability of taste bud organoids attached to the tips of the microelectrode. This enhances the success rate of MEA chips in producing responsive signals from taste bud organoids upon taste stimuli.

An image of the MEA chip used in this study is shown in Figure 3a, which consists of a square glass substrate fixed with a round cell culture chamber divided into six sector areas. The culture chamber allows for the loading of taste bud organoids to the surface of MEA chips, where the surfaces of microelectrodes were exposed to the solution loaded to the culture chamber. Next, the prepared taste bud organoids were transferred to the surface of the MEA chip for coupling via 24 h incubation. During this process, cells of organoids adhere to MEA surfaces perhaps via the cytoskeleton [44], membrane-bound adhesion proteins [45], and glyocalyx elements [46]. This allows for the good attachment of taste bud organoids onto the surface of MEA chips. The area indicated by the red arrow is the electrode that detects the membrane potential. The resultant taste bud organoids attached to the MEA chip are depicted in Figure 3b, which shows that taste bud organoids were randomly attached to the chip surface and maintained the original multicellular structure.

In addition, some taste bud organoids were attached to the surfaces of the individual circular microelectrode. This made it possible for the microelectrode to record membrane potential changes from the attached taste bud organoids. These results suggested that high-efficient coupling between taste bud organoids and MEA chips was obtained and that it is suitable to be used for further experiments related to performance testing.

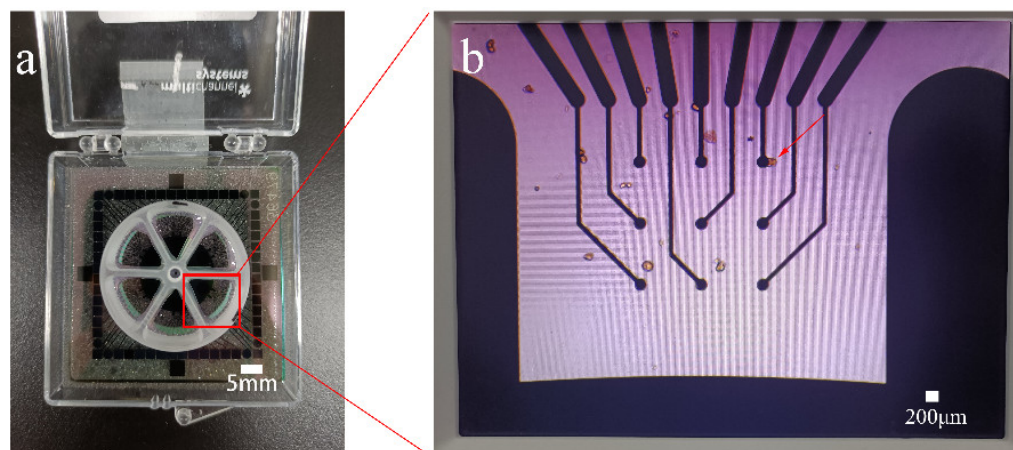


**Figure 3.** (a) An image of the MEA chip. (b) A chip surface after culturing the taste bud organoids for 24 h.

### 3.3. Performance Testing of Taste Bud Organoid-Based Biosensors

To preliminarily test the performance of this taste bud organoid-based MEA biosensor, we first recorded the signals from the taste bud organoids using an MEA chip when no taste stimuli were applied. The recorded results from one typical channel of the MEA chip are shown in Figure 4a, which represent those microelectrodes attached with taste bud organoids. The left column of Figure 4 presents the original signal recordings, showing the typical extracellular recordings of taste bud spheroids by a microelectrode of an MEA chip upon the spontaneous status and stimulation status. Extracellular action potentials recorded by MEAs are also known as “spikes” [47]. The voltage-dependent sodium channel is responsible for the rising phase of an action potential.  $\text{Ca}^{2+}$  and  $\text{K}^{+}$  affect the descending phase of the action potential [48]. These results indicated that the microelectrodes efficiently recorded the specific firing patterns of spikes from taste cells under different stimulation statuses. This suggests that taste bud spheroids immobilized on the MEA surface are capable of responding to taste stimulations. The right column of Figure 4 shows the results of clustering of the recorded spikes from the original recordings using a Butterworth low-cut Filter with a 250-Hz cutoff frequency and a scroll range of 100. Then, signal spike times with similar waveforms were collected (and displayed). The originally recorded spikes indicated that the taste spheroid is responsive to the taste stimuli. These spikes at certain firing rates are probably due to the spontaneous firing of taste bud organoids. This could be considered the baseline of the taste bud organoid-based biosensor since it was recorded when no taste stimuli were applied to the detection chamber (Figure 4a). On the contrary, some channels of the MEA chip did not record any spikes, which is probably due to the lack of taste bud organoids attached to the tip of the microelectrode. More importantly, the distribution of taste bud organoids on the MEA chip surface was at a high density, which makes it possible to achieve highly-efficient coupling between taste bud organoids and the MEA chip. In our experiments, more than 60% of channels of the MEA chip could record the baseline successfully. This means more than 60% of microelectrodes were successfully coupled with taste bud organoids.

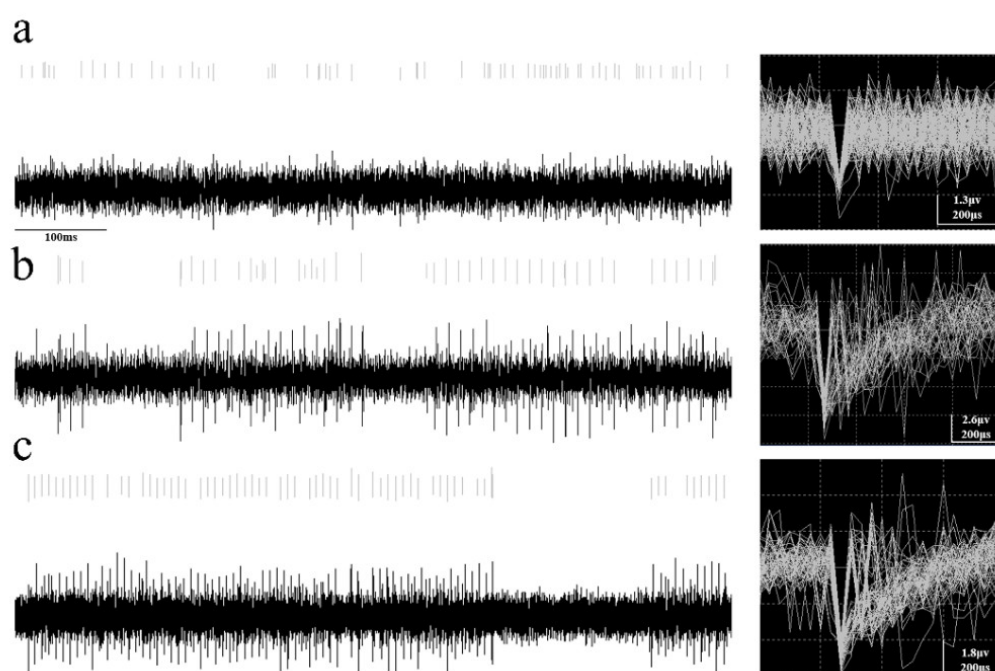


**Figure 4.** Membrane potential changes were recorded from attached taste bud organoids via the MEA chip (a) when no stimulus, (b) acid stimulus (10 mM citric acid), and (c) salty stimulus (100 mM NaCl) were applied separately. The left column presents the original recording signals, showing the patterns of firing spikes via grating. The right column shows the results of the clustering of recorded spikes from the original recordings.

To further verify the responsive capabilities of taste bud organoids attached to the MEA chips, various taste stimuli (10 mM citric acid and 100 mM NaCl) were applied to stimulate taste bud organoids. For this, sour and salty stimuli were introduced to the detection chamber loaded with taste bud organoids separately. The MEA recording results are shown in Figure 4b,c. Compared with the spontaneous generation state (Figure 4a) which had no obvious waveform changes on either side of the spike, MEA chips recorded specific spikes under the stimulation of sour and salty substances (Figure 4b,c), showing a smooth rising waveform on the right side of the spike. These distinct waveforms could be elicited when taste stimuli were applied. These results suggest that the attached taste bud organoids can respond to taste stimuli. In addition, the waveform changes caused by different taste stimuli could be used to distinguish the types of taste stimuli in the future. It is interesting that all the channels loaded with taste bud organoids responded to both sour and salty stimuli and showed responsive signals. These results indicate that the prepared taste bud organoids have a responsive capability to taste stimuli, which suggests a good homogeneity of prepared taste bud organoids, to some extent, when utilized as sensitive elements for the development of biosensors toward taste sensation. Then, at every 2 s, the number of spikes generated within the channel where the response occurred was counted. GraphPad software was used to map and obtain the quantitative results of the spike (Figure 5). The results prove that these taste bud organoid-based MEA biosensors have great potential to provide novel tools for the research of taste sensation mechanisms as well as for the detection of specific taste substances. However, further testing and improvement on the taste sensation capabilities of this biosensor are necessary to enhance the recording efficiencies of potential changes from loaded taste bud organoids onto MEA chips.

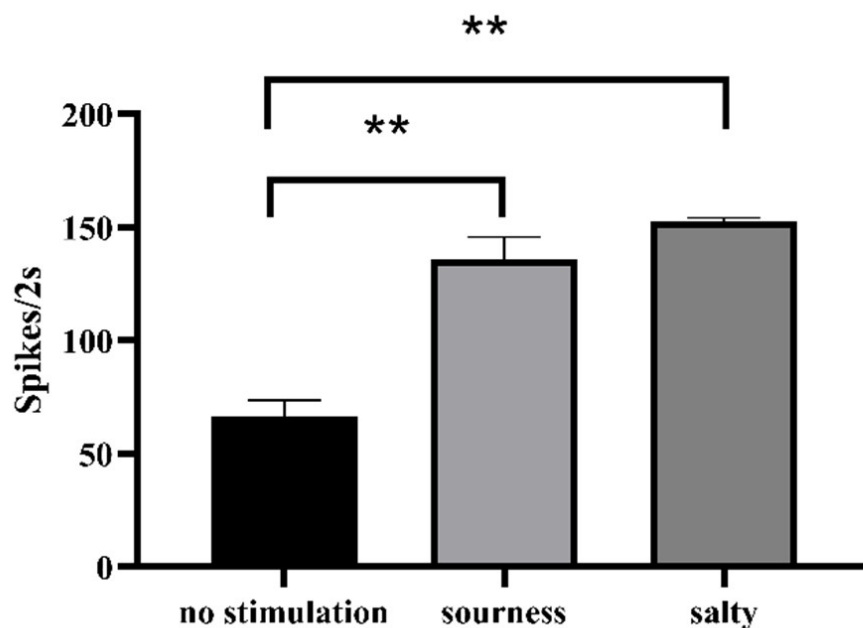


**Figure 5.** Spike responses of taste bud organoids are stimulated by different taste substances. All data represent the mean  $\pm$  standard error of the mean (S.E.M.) and are shown in a histogram. \*\*  $p < 0.01$  is considered as significant difference, Student's t-test.

#### 4. Conclusions

In this study, a taste bud organoid-based MEA biosensor was developed for taste sensation. We investigated the preparation of functional taste bud organoids from the taste stem/progenitor cells isolated from the lingual epithelium of neonatal mice. The taste bud organoids were shown to be suitable for use as sensitive elements for the development of a taste bud organoid-based biosensor for taste stimuli detection; 64-channel MEA chips were utilized as transducers. These taste bud organoids were coupled to MEA chips to monitor the electrophysiological signals from taste bud organoids in response to various taste stimuli. The waveform changes were caused by taste stimuli when compared to no stimulation. This taste bud organoid-based biosensor has great potential in providing a new method for the study of taste sensation mechanisms as well as in the detection of specific taste substances. However, more attempts to tune the stability of the system are necessary to improve the performance of this biosensor. In the future, we will focus on the improvement of the quality of recorded signals from taste bud organoids as well as the coupling efficiency between taste bud organoids and MEA chips.

**Author Contributions:** S.L.: conceptualization, investigation, writing—original draft preparation, writing—review, and editing; P.Z.: software, investigation, visualization; Y.T.: software, visualization; Y.C.: visualization; Y.L.: software; M.W.: investigation, W.C.: writing—review and editing, software; L.D.: conceptualization, writing—review and editing, supervision, funding acquisition; C.W.: writing—review and editing, supervision, funding acquisition, project administration. All authors have read and agreed to the published version of the manuscript.

**Funding:** This research was funded by grants from the National Natural Science Foundation of China (grant numbers 32071370, 51861145307, and 31700859), and the Key Research and Development Program of Shaanxi Province-International Science and Technology Cooperation General Project (grant number 2022KW-23).

**Institutional Review Board Statement:** The animal study protocol was approved by Biomedical Ethics Committee of the Medical Department of Xi'an Jiaotong University (protocol code: 2020-1014 and date of approval: 3 April 2020).

**Informed Consent Statement:** Not applicable.

**Data Availability Statement:** No new data were created or analyzed in this study. Data sharing is not applicable to this article.

**Conflicts of Interest:** The authors declare no conflict of interest.

## References

1. Barlow, L.A. Progress and renewal in gustation: New insights into taste bud development. *Development* **2015**, *142*, 3620–3629. [[CrossRef](#)] [[PubMed](#)]
2. Gardiner, J.; Barton, D.; Vanslambrouck, J.M.; Braet, F.; Hall, D.; Marc, J.; Overall, R. Defects in tongue papillae and taste sensation indicate a problem with neurotrophic support in various neurological diseases. *Neurosci. Rev. J. Bringing Neurobiol. Neurol. Psychiatr.* **2008**, *14*, 240–250. [[CrossRef](#)] [[PubMed](#)]
3. Gao, X.; Wu, Y.; Liao, L.; Tian, W. Oral Organoids: Progress and Challenges. *J. Dent. Res.* **2021**, *100*, 454–463. [[CrossRef](#)] [[PubMed](#)]
4. Kalmykov, A.; Huang, C.; Bliley, J.; Shiwarski, D.; Tashman, J.; Abdullah, A.; Rastogi, S.K.; Shukla, S.; Mataev, E.; Feinberg, A.W.; et al. Organ-on-a-chip: Three-dimensional self-rolled biosensor array for electrical interrogations of human electrogenic spheroids. *Sci. Adv.* **2019**, *5*, eaax0729. [[CrossRef](#)] [[PubMed](#)]
5. Lee, J.S.; Cho, A.N.; Jin, Y.; Kim, J.; Kim, S.; Cho, S.W. Bio-artificial tongue with tongue extracellular matrix and primary taste cells. *Biomaterials* **2018**, *151*, 24–37. [[CrossRef](#)]
6. Qiu, C.; Cui, C.; Hautefort, C.; Haehner, A.; Zhao, J.; Yao, Q.; Zeng, H.; Nisenbaum, E.J.; Liu, L.; Zhao, Y.; et al. Olfactory and Gustatory Dysfunction as an Early Identifier of COVID-19 in Adults and Children: An International Multicenter Study. *Otolaryngol. Head Neck Surg.* **2020**, *163*, 714–721. [[CrossRef](#)]
7. Barker, K.E.; Batstone, M.D.; Savage, N.W. Comparison of treatment modalities in burning mouth syndrome. *Aust. Dent. J.* **2009**, *54*, 300–305. [[CrossRef](#)]
8. Hampf, G.; Aalberg, V.; Sundén, B. Experiences from a facial pain unit. *J. Craniomandib. Disord. Facial Oral Pain* **1990**, *4*, 267–272.
9. Yun, J.; Cho, A.N.; Cho, S.W.; Nam, Y.S. DNA-mediated self-assembly of taste cells and neurons for taste signal transmission. *Biomater. Sci.* **2018**, *6*, 3388–3396. [[CrossRef](#)]
10. Deshpande, D.A.; Wang, W.C.; McIlmoyle, E.L.; Robinett, K.S.; Schillinger, R.M.; An, S.S.; Sham, J.S.; Liggett, S.B. Bitter taste receptors on airway smooth muscle bronchodilate by localized calcium signaling and reverse obstruction. *Nat. Med.* **2010**, *16*, 1299–1304. [[CrossRef](#)]
11. Ren, W.; Lewandowski, B.C.; Watson, J.; Aihara, E.; Iwatsuki, K.; Bachmanov, A.A.; Margolskee, R.F.; Jiang, P. Single Lgr5- or Lgr6-expressing taste stem/progenitor cells generate taste bud cells ex vivo. *Proc. Natl. Acad. Sci. USA* **2014**, *111*, 16401–16406. [[CrossRef](#)] [[PubMed](#)]
12. Guo, Q.; Chen, S.; Rao, X.; Li, Y.; Pan, M.; Fu, G.; Yao, Y.; Gao, X.; Tang, P.; Zhou, Y.; et al. Inhibition of SIRT1 promotes taste bud stem cell survival and mitigates radiation-induced oral mucositis in mice. *Am. J. Transl. Res.* **2019**, *11*, 4789–4799. [[PubMed](#)]
13. Drost, J.; Clevers, H. Organoids in cancer research. *Nat. Rev. Cancer* **2018**, *18*, 407–418. [[CrossRef](#)]
14. Lacroix, J.J.; Campos, F.V.; Frezza, L.; Bezanilla, F. Molecular bases for the asynchronous activation of sodium and potassium channels required for nerve impulse generation. *Neuron* **2013**, *79*, 651–657. [[CrossRef](#)]
15. Cummings, T.A.; Daniels, C.; Kinnamon, S.C. Sweet taste transduction in hamster: Sweeteners and cyclic nucleotides depolarize taste cells by reducing a K<sup>+</sup> current. *J. Neurophysiol.* **1996**, *75*, 1256–1263. [[CrossRef](#)] [[PubMed](#)]
16. Avenet, P.; Lindemann, B. Noninvasive recording of receptor cell action potentials and sustained currents from single taste buds maintained in the tongue: The response to mucosal NaCl and amiloride. *J. Membr. Biol.* **1991**, *124*, 33–41. [[CrossRef](#)] [[PubMed](#)]
17. Miyamoto, T.; Fujiyama, R.; Okada, Y.; Sato, T. Sour transduction involves activation of NPPB-sensitive conductance in mouse taste cells. *J. Neurophysiol.* **1998**, *80*, 1852–1859. [[CrossRef](#)] [[PubMed](#)]
18. Furue, H.; Yoshii, K. In situ tight-seal recordings of taste substance-elicited action currents and voltage-gated Ba currents from single taste bud cells in the peeled epithelium of mouse tongue. *Brain Res.* **1997**, *776*, 133–139. [[CrossRef](#)]
19. Roper, S.D.; Chaudhari, N. Taste buds: Cells, signals and synapses. *Nat. Rev. Neurosci.* **2017**, *18*, 485–497. [[CrossRef](#)]
20. Rössler, P.; Kroner, C.; Freitag, J.; Noè, J.; Breer, H. Identification of a phospholipase C beta subtype in rat taste cells. *Eur. J. Cell Biol.* **1998**, *77*, 253–261. [[CrossRef](#)]
21. Miyoshi, M.A.; Abe, K.; Emori, Y. IP(3) receptor type 3 and PLCbeta2 are co-expressed with taste receptors T1R and T2R in rat taste bud cells. *Chem. Senses* **2001**, *26*, 259–265. [[CrossRef](#)] [[PubMed](#)]
22. Zhang, Z.; Zhao, Z.; Margolskee, R.; Liman, E. The transduction channel TRPM5 is gated by intracellular calcium in taste cells. *J. Neurosci.* **2007**, *27*, 5777–5786. [[CrossRef](#)] [[PubMed](#)]
23. Du, L.; Wang, J.; Chen, W.; Zhao, L.; Wu, C.; Wang, P. Dual functional extracellular recording using a light-addressable potentiometric sensor for bitter signal transduction. *Anal. Chim. Acta* **2018**, *1022*, 106–112. [[CrossRef](#)] [[PubMed](#)]
24. Liu, Q.; Zhang, F.; Zhang, D.; Hu, N.; Hsia, K.J.; Wang, P. Extracellular potentials recording in intact taste epithelium by microelectrode array for a taste sensor. *Biosens. Bioelectron.* **2013**, *43*, 186–192. [[CrossRef](#)]
25. Ahn, S.R.; An, J.H.; Song, H.S.; Park, J.W.; Lee, S.H.; Kim, J.H.; Jang, J.; Park, T.H. Duplex Bioelectronic Tongue for Sensing Umami and Sweet Tastes Based on Human Taste Receptor Nanovesicles. *ACS Nano* **2016**, *10*, 7287–7296. [[CrossRef](#)]

26. Wang, J.; Kong, S.; Chen, F.; Chen, W.; Du, L.; Cai, W.; Huang, L.; Wu, C.; Zhang, D.W. A bioelectronic taste sensor based on bioengineered *Escherichia coli* cells combined with ITO-constructed electrochemical sensors. *Anal. Chim. Acta* **2019**, *1079*, 73–78. [[CrossRef](#)]
27. Son, M.; Kim, D.; Ko, H.J.; Hong, S.; Park, T.H. A portable and multiplexed bioelectronic sensor using human olfactory and taste receptors. *Biosens. Bioelectron.* **2017**, *87*, 901–907. [[CrossRef](#)]
28. Wu, C.; Du, L.; Zou, L.; Huang, L.; Wang, P. A biomimetic bitter receptor-based biosensor with high efficiency immobilization and purification using self-assembled aptamers. *Analyst* **2013**, *138*, 5989–5994. [[CrossRef](#)]
29. Chen, J.; Wise, K.D.; Hetke, J.F.; Bledsoe, S.C., Jr. A multichannel neural probe for selective chemical delivery at the cellular level. *IEEE Trans. Bio-Med. Eng.* **1997**, *44*, 760–769. [[CrossRef](#)]
30. Takeuchi, S.; Ziegler, D.; Yoshida, Y.; Mabuchi, K.; Suzuki, T. Parylene flexible neural probes integrated with microfluidic channels. *Lab Chip* **2005**, *5*, 519–523. [[CrossRef](#)]
31. McCall, J.G.; Qazi, R.; Shin, G.; Li, S.; Ikram, M.H.; Jang, K.I.; Liu, Y.; Al-Hasani, R.; Bruchas, M.R.; Jeong, J.W.; et al. Preparation and implementation of optofluidic neural probes for in vivo wireless pharmacology and optogenetics. *Nat. Protoc.* **2017**, *12*, 219–237. [[CrossRef](#)] [[PubMed](#)]
32. Blanche, T.J.; Spacek, M.A.; Hetke, J.F.; Swindale, N.V. Polytrodes: High-density silicon electrode arrays for large-scale multiunit recording. *J. Neurophysiol.* **2005**, *93*, 2987–3000. [[CrossRef](#)] [[PubMed](#)]
33. Obien, M.E.; Deligkaris, K.; Bullmann, T.; Bakkum, D.J.; Frey, U. Revealing neuronal function through microelectrode array recordings. *Front. Neurosci.* **2014**, *8*, 423. [[CrossRef](#)]
34. Lebreton, F.; Pirog, A.; Belouah, I.; Bosco, D.; Berney, T.; Meda, P.; Bornat, Y.; Catargi, B.; Renaud, S.; Raoux, M.; et al. Slow potentials encode intercellular coupling and insulin demand in pancreatic beta cells. *Diabetologia* **2015**, *58*, 1291–1299. [[CrossRef](#)]
35. Hennig, M.H.; Hurwitz, C.; Sorbaro, M. Scaling Spike Detection and Sorting for Next-Generation Electrophysiology. *Adv. Neurobiol.* **2019**, *22*, 171–184. [[CrossRef](#)]
36. Takekawa, T.; Isomura, Y.; Fukai, T. Spike sorting of heterogeneous neuron types by multimodality-weighted PCA and explicit robust variational Bayes. *Front. Neuroinform.* **2012**, *6*, 5. [[CrossRef](#)] [[PubMed](#)]
37. Quiroga, R.Q.; Nadasdy, Z.; Ben-Shaul, Y. Unsupervised spike detection and sorting with wavelets and superparamagnetic clustering. *Neural Comput.* **2004**, *16*, 1661–1687. [[CrossRef](#)] [[PubMed](#)]
38. Thomas, C.A., Jr.; Springer, P.A.; Loeb, G.E.; Berwald-Netter, Y.; Okun, L.M. A miniature microelectrode array to monitor the bioelectric activity of cultured cells. *Exp. Cell Res.* **1972**, *74*, 61–66. [[CrossRef](#)]
39. Pine, J. Recording action potentials from cultured neurons with extracellular microcircuit electrodes. *J. Neurosci. Methods* **1980**, *2*, 19–31. [[CrossRef](#)]
40. Delgado Ruz, I.; Schultz, S.R. Localising and classifying neurons from high density MEA recordings. *J. Neurosci. Methods* **2014**, *233*, 115–128. [[CrossRef](#)]
41. Ren, W.; Liu, Q.; Zhang, X.; Yu, Y. Age-related taste cell generation in circumvallate papillae organoids via regulation of multiple signaling pathways. *Exp. Cell Res.* **2020**, *394*, 112150. [[CrossRef](#)] [[PubMed](#)]
42. Kinnamon, S.C. Taste receptor signalling from tongues to lungs. *Acta Physiol.* **2012**, *204*, 158–168. [[CrossRef](#)] [[PubMed](#)]
43. Le Gléau, L.; Rouault, C.; Osinski, C.; Prifti, E.; Soula, H.A.; Debédât, J.; Busieau, P.; Amouyal, C.; Clément, K.; Andreelli, F.; et al. Intestinal alteration of  $\alpha$ -gustducin and sweet taste signaling pathway in metabolic diseases is partly rescued after weight loss and diabetes remission. *Am. J. Physiology. Endocrinol. Metab.* **2021**, *321*, E417–E432. [[CrossRef](#)] [[PubMed](#)]
44. Parsons, J.T.; Horwitz, A.R.; Schwartz, M.A. Cell adhesion: Integrating cytoskeletal dynamics and cellular tension. *Nat. Rev. Mol. Cell Biol.* **2010**, *11*, 633–643. [[CrossRef](#)] [[PubMed](#)]
45. Kanchanawong, P.; Shtengel, G.; Pasapera, A.M.; Ramko, E.B.; Davidson, M.W.; Hess, H.F.; Waterman, C.M. Nanoscale architecture of integrin-based cell adhesions. *Nature* **2010**, *468*, 580–584. [[CrossRef](#)] [[PubMed](#)]
46. Paszek, M.J.; DuFort, C.C.; Rossier, O.; Bainer, R.; Mouw, J.K.; Godula, K.; Hudak, J.E.; Lakins, J.N.; Wijekoon, A.C.; Cassereau, L.; et al. The cancer glycocalyx mechanically primes integrin-mediated growth and survival. *Nature* **2014**, *511*, 319–325. [[CrossRef](#)]
47. Lewis, C.M.; Bosman, C.A.; Fries, P. Recording of brain activity across spatial scales. *Curr. Opin. Neurobiol.* **2015**, *32*, 68–77. [[CrossRef](#)]
48. Vatanparast, J.; Khalili, S.; Naseh, M. Dual effects of eugenol on the neuronal excitability: An in vitro study. *Neurotoxicology* **2017**, *58*, 84–91. [[CrossRef](#)]